Available online at www.sciencedirect.com
SCIENCE DIRECT®
International Journal of Heat and Mass Transfer 48 (2005) 4811–4828
International Journal of HEAT and MASS TRANSFER
www.elsevier.com/locate/ijhmt

Numerical simulation of steady flow fields in coiled flow inverter

Vimal Kumar, K.D.P. Nigam *

Department of Chemical Engineering, Indian Institute of Technology, Delhi, Hauz Khas, New Delhi 110 016, India

Received 11 August 2004; received in revised form 5 May 2005
Available online 19 August 2005

Abstract

Flatter velocity profiles and more uniform thermal environments are extremely desirous factors for improved performance in flow reactors and heat exchangers. One means of achieving it in laminar flow systems is to use mixers and flow inverters. In the present study a new device is introduced based on the flow inversion by changing the direction of centrifugal force in helically coiled tubes. The objective of the present study is to characterize flow development and temperature fields in the proposed device made up from the configurations of bent coils. The main mechanism generating the flow is the production of spatially chaotic path by changing the direction of flow using a 90° bend in helical coils (alternating Dean flow). If the direction of centrifugal force is rotated by any angle, the plane of vortex formation also rotates with the same angle. Thus in helical flow a 90° shift in the direction of centrifugal force cause a complete flow inversion. Complete flow fields and thermal fields in helical coil and bent coil configuration were studied using computational fluid dynamics software (FLUENT 6.0). The three-dimensional governing equations for momentum and energy under the laminar flow conditions were solved with a control-volume finite difference method (CVFDM) with second-order accuracy. The flow pattern obtained for the helical coil was in good agreement to those observed by the previous investigators [S.W. Jones, O.M. Thomas, H. Aref, Chaotic advection by laminar flow in twisted pipe. J. Fluid Mech. 209 (1989) 335–357; Ch. Duchene, H. Peerhossaini, P.J. Michard, On the velocity field and tracer patterns in a twisted duct flow. Phys. Fluids 7 (1995) 1307–1317]. The comparison of the flow fields and temperature fields in the helical tube and bent coil configuration are discussed. The bent coil configuration shows a 20–30% enhancement in the heat transfer due to chaotic mixing while relative pressure drop is 5–6%. The results of the present study can be used to model transport processes for developing flows in curved tubes such as chromatographic columns (less axial dispersion [A.K. Saxena, K.D.P. Nigam, Coiled configuration for flow inversion and its effect on residence time distribution. AIChE J. 30 (1984) 363–368]), Chemical reactors (narrower RTD), heat transfer devices, and some biomedical devices.

Keywords: Heat transfer; Helical tube; Bent coils; CFD

* Corresponding author. Tel.: +91 11 2659 1020/6178; fax: +91 11 2659 1020.
E-mail address: nigamkdp@gmail.com (K.D.P. Nigam).

0017-9310/$ - see front matter © 2005 Elsevier Ltd. All rights reserved.
doi:10.1016/j.ijheatmasstransfer.2005.05.037

Nomenclature

a	radius of the helical pipe, m
A	area, m^2
C_p	specific heat, kJ/(kg K)
d_h	hydraulic diameter of the helical pipe (=2a), m
H	pitch, m
k	thermal conductivity, W/(m K)
n	coordinate direction perpendicular to a surface
p	pressure, N/m^2
q	heat flux, $W\,m^{-2}$
R_c	radius of the coil, m
N_{Re}	Reynolds number ($=\rho U_0 d_h/\mu$)
N_{Pr}	Prandtl number
N_{Nu}	Nusselt number
T	temperature, K
T_b	fluid bulk temperature on one cross-section $\left(\frac{1}{u_s A}\int_0^A u_s T\,dA\right)$, K
U_0	inlet velocity, m/s
u_i	velocity component in i-direction (i = 1, 2, 3), m/s
u_s	axial velocity component, m/s
U_s	non-dimensional axial velocity (u_s/U_0)
U_{2nd}	non-dimensional secondary velocity
x	spatial position, m
x_i	master Cartesian coordinate in i-direction (i = 1, 2, 3), m

Greek symbols

α	angle, degree
δ	curvature ratio (a/R_c)
δ_{ij}	Dirac delta function
Θ	non-dimensional temperature, $\frac{T_w - T_0}{T_b - T_w}$
ρ	density of fluid, kg/m^3

Subscripts

0	inlet conditions
2nd	secondary flow
b	bulk quantity
w	wall condition

1. Introduction

Flow and heat transfer in helical pipes with a constant circular or rectangular cross-section has been a topic of important fundamental engineering interests during the past decades. Berger et al. [3] and Shah and Joshi [4] have presented extensive reviews of fluid flow and heat transfer in helical pipes. Helically coiled tubes are simple and effective means of augmenting heat and mass transfer in a wide variety of industrial applications ranging from stagnant batch heating and cooling to dynamic distillation processes. In the helically coiled tubes, the modification of the flow is due to the centrifugal forces (Dean roll cells [5,6]) caused by the curvature of the tube, which produce a secondary flow field with a circulatory motion pushing the fluid particles toward the core region of the tube. Because of the stabilizing effects of this secondary flow, laminar flow persists too higher Reynolds number value in helical coils as compared to straight tubes. Consequently, the differences in heat and mass transfer performance between coils and straight tubes are particularly distinct in the laminar flow region. In fact, there is global heat transfer enhancement, but Raju and Rathna [7] showed that in helical coiled tube the isotherms of temperature for different kinds of fluids contain segregated cold and hot regions. The Dean roll cells divide the cross-section into two zones in each of which the isotherms forms the closed curves. Fluid particles inside the Dean roll cells are prevented from approaching the hot walls; thus mixing is poor, giving rise to a heterogeneous temperature field. To overcome this phenomenon, Jones et al. [1], Acharya et al. [12] and Peerhossaini et al. [8] presented an alternative regime in laminar flow that has dispersive properties close to the turbulent regime. This phenomenon, called chaotic advection or Langrangian turbulence, is analogous to temporal chaos in which a small number of degrees of freedom can cause chaotic evolution over time. In chaotic advection, the fluid-particle trajectories are chaotic and enhance mixing, consequently increasing heat transfer. Such tools were addressed in Mokrani et al. [9]. The details of the chaotic and temporal flows are discussed in [8–21].

Acharya et al. [12,13] numerically showed that the mixing can be enhanced, by inserting a geometrical perturbation (by alternating sequence of bends) in the laminar flow. This perturbation is achieved by merely shifting each bend by an angle, χ between 0° and 90°. They have solved the problem numerically by using analytical flow field obtained by Dean. The energy equation, though linear is solved numerically, using Dean's velocity fields, to give the temperature distribution and heat transfer characteristics. They also reported that in the alternating axis coil, the temperature field becomes flatter than in helical coil. Duchene et al. [2] analyzed the formation and reorganization of Dean roll cells under abrupt curvature change in a twisted square duct.

Acharya et al. [12] experimentally studied the heat transfer enhancement in a chaotic coil, made of 180° bends, immersed in a constant temperature bath. Experiments were run for N_{Re} ranging from 3000 to 10,000. They observed an increase of 6–8% of inner heat transfer coefficient at high Reynolds numbers and the relative pressure drop was 1.5–2.5%. Mokrani et al. [9] proposed a similar kind of equipment but the geometry was slightly different from that of [12]: half circle elements were repeated with 90° angle between every two adjacent element. They reported the enhancement in heat transfer from 13% to 28%. The difference in heat transfer enhancement with Acharya et al. [12] was due to the low Reynolds number and high Prandtl number (CMC). Acharya et al. [12] and Mokrani et al. [9], both reported that Reynolds number and Prandtl number have same effect on heat transfer.

Saxena and Nigam [22,23] proposed a new technique, "bending of helical coils", to cause multiple flow inversion at low flow rates. For the case of fully developed secondary flow, a 90° bend induces a flow inversion, which narrows the RTD for equal arm lengths before and after the bend. They presented that the narrowest value of RTD (0.86) with a unit having 57 bends, and for the same unit the axial dispersion reduces 20 times than in helical tubes. Chaotic flow in this geometry is generated as follows: in laminar flow inside a coiled tube, centrifugal forces lead to the generation of a secondary transverse flow, generally called Dean roll-cells, as shown in Fig. 1(a). In the alternating Dean flow (Fig. 1(b)), a 90° bend introduced between the two helical tubes; this makes the roll-cells regenerate in a plane perpendicular to the previous one, due to the reorientation of the centrifugal forces. This geometrical perturbation is the main cause of radial mixing.

The focus of this work is to characterize flow development and temperature fields in coiled flow inverter. The most important information in the design of the helical coil device is the pressure drop and the heat-transfer coefficient. Therefore, hydrodynamics and thermal development studies were conducted, using Newtonian fluid, for a range of Reynolds numbers from 25 to 400. A brief description of the fluid flow in curved channels and its modification arising due to the change in the direction of the curvature plane in helical coil is presented. All the computations were carried out on a SUN Blade 2000 computer in the Chemical Reaction Engineering Laboratory at Indian Institute of Technology, Delhi.

2. Mathematical formulation

2.1. Governing equations

The geometry considered and the system of the coordinates is illustrated in Fig. 2. The circular pipe has a diameter of $2a$, and is coiled at a radius R_c, while the distance between the two turns (the pitch) is reported by p. The bends introduced in between the helical coils are of 90° and each helical tube has same length before and after the bend. In the present study, the Cartesian coordinate system (x, y, z) is used to

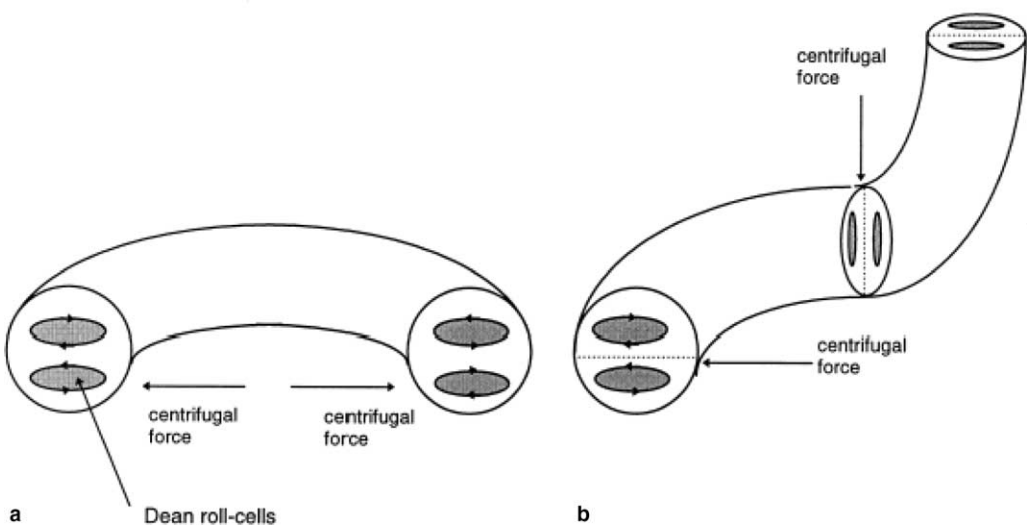

Fig. 1. Generation of spatially chaotic particle paths in three-dimensional steady, laminar flow. (a) Regular Dean flow and (b) alternate Dean flow.

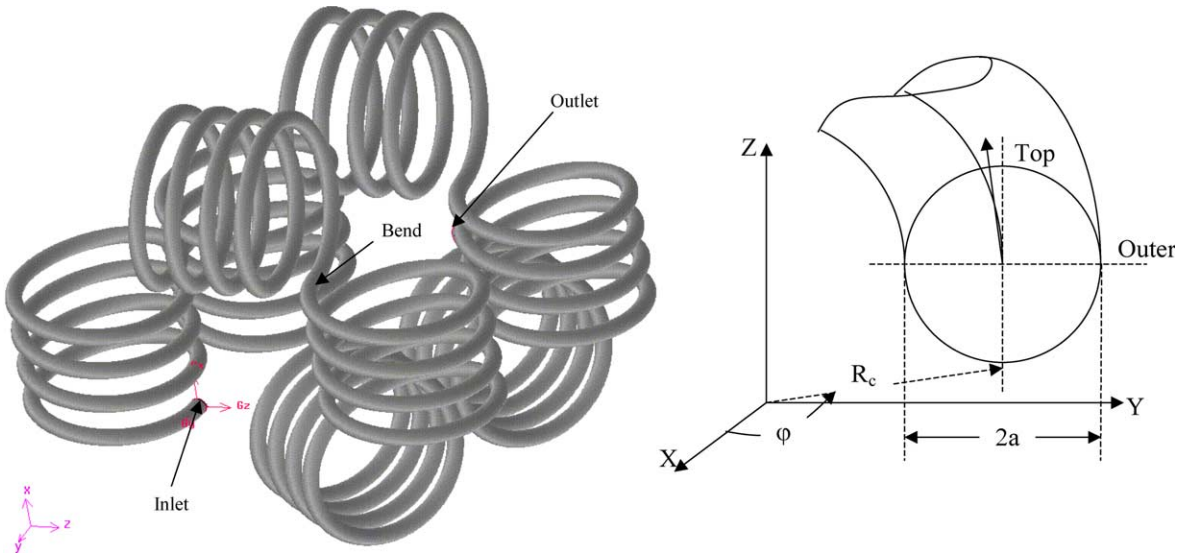

Fig. 2. Schematic geometry and coordinates of the bent helix.

represent the coiled flow inverter in numerical simulation. At the inlet ($\varphi = 0$), fluid enters at a temperature T_0 with a velocity of U_0. The wall of the pipe is heated under constant temperature T_w. The laminar flow and heat transfer develop simultaneously down-stream in the helical pipe. The flow is considered to be steady, and constant thermal properties are assumed. The differential equations governing the three-dimensional laminar flow in the coiled flow inverter could be written in tensor form in the master Cartesian coordinate system as

Continuity:

$$\frac{\partial u_i}{\partial x_i} = 0 \tag{1}$$

Momentum:

$$\frac{\partial}{\partial x_j}\left[\mu\left(\frac{\partial u_i}{\partial x_j}+\frac{\partial u_j}{\partial x_i}\right) - \rho u_j u_i - \delta_{ij} p\right] + \rho g_i = 0 \tag{2}$$

Energy:

$$\frac{\partial}{\partial x_j}\left[k\left(\frac{\partial T}{\partial x_j} - \rho u_j C_p T\right) + \mu \Phi_v\right] = 0 \tag{3}$$

where $\mu\Phi_v$ is the viscous heating term in energy equation, and Φ_v is represented by

$$\Phi_v = \frac{\partial u_i}{\partial x_j}\left(\frac{\partial u_i}{\partial x_j}+\frac{\partial u_j}{\partial x_i} - \frac{2}{3}\mu\frac{\partial u_i}{\partial u_j}\delta_{ij}\right) \tag{4}$$

2.2. Boundary conditions

No-slip boundary condition, $u_i = 0$, and constant temperature, T_w, are imposed on the wall. At the inlet, a fully developed duct flow velocity profiles and a fixed pressure at the outlet of the coiled flow inverter were employed.

The diffusion flux at the outlet for all variables in the exit direction is set to zero

$$\frac{\partial}{\partial n}(u_i, p, T) = 0 \tag{5}$$

where n is used to represent the normal coordinate direction perpendicular to the outlet plane.

2.3. Parameter definitions

To represent the results and characterize the heat transfer in coiled flow inverter, the following non-dimensional variables and parameters are used:

$$N_{Re} = \frac{\rho u_0 d_i}{\mu} \tag{6a}$$

$$\lambda = \frac{d_C}{d_i} \tag{6b}$$

$$\Theta = \frac{T - T_w}{T_b - T_w} \tag{6c}$$

$$T_b = \left(\frac{1}{\overline{u_s} A}\int_0^A u_s T \, dA\right) \tag{6d}$$

$$f_\theta = \frac{\tau_w}{\frac{1}{2}\rho U_0^2}, \quad f_m = \frac{1}{2\pi}\int_0^{2\pi} f_\theta \, d\theta \tag{6e}$$

$$N_{Nu,\theta} = \frac{q_w d_h}{k(T_w - T_b)}, \quad N_{Nu,m} = \frac{1}{\overline{u_s} A}\int_0^A N_{Nu,\theta} \, d\theta \tag{6f}$$

where λ is the curvature ratio and T_b is the bulk temperature, f_θ and $N_{Nu,\theta}$, local friction factor and Nusselt

number along the circumference of the pipe, respectively; f_m and $N_{Nu,m}$, the circumference average friction average friction factor and Nusselt number. U_0 denotes the velocity at the inlet of the tube.

3. Numerical computation

3.1. Numerical method

The governing equations for heat transfer in the helical pipe were solved in the master Cartesian coordinate system with a control-volume finite difference method (CVFDM) similar to that introduced by Patankar [25]. Fluent program [26] is used as a numerical solver for the present three-dimensional simulation.

3.2. Grid system

An unstructured (block-structured) non-uniform grid system is used to discretize the governing equations. Fig. 3 illustrates the grid topology used on one cross-section and a typical hexahedral element for the three-dimensional grid system.

The convection term in the governing equations was modeled with the bounded second-order upwind scheme and the diffusion term was computed using the multilinear interpolating polynomials nodes $N_i(X, Y, Z)$. The final discrete algebraic equation for variable ϕ at each node is a set of nominally linear equations that can be written as

$$a_p\phi_p = \sum_{nb} a_{nb}\phi_{nb} + C_{sb} \tag{7}$$

where a_p is the center coefficient; a_{nb} is the influence coefficient for the neighbour; and C_{sb} is the contribution of the constant part of the source term S_C in $S = S_C + C_{ps}$ and of the boundary conditions. The SIMPLE algorithm [25] is used to resolve the coupling between velocity and pressure. To accelerate the convergence, the under-relaxation factor for the pressure, p, is 0.3; that for temperature, T is 0.9; that for the velocity component in the i-direction, u_i, is 0.5; and that for body force is 0.8.

3.3. Convergence criteria

The numerical computation is considered converged when the residual summed over all the computational nodes at nth iteration, R^n_ϕ, satisfies the following criterion:

$$\frac{R^n_\phi}{R^m_\phi} \leqslant 10^{-5} \tag{8}$$

where R^m_ϕ denotes the maximum residual value of ϕ variable after m iterations, ϕ applied for p, u_i, and for T.

A grid refinement study was conducted to determine an adequate distribution. Table 1 presents a comparison

Table 1
Grid independent tests ($N_{Re} = 316$, $N_{Pr} = 7$, and $\delta = 0.1$)

Total grids	$N_{Nu,\theta}$	$N_{Nu,m}$	f_m
500×200	18.65	11.15	0.0776
624×200	18.80	11.27	0.0772
500×240	18.72	11.21	0.0774
896×240	18.718	11.21	0.0774

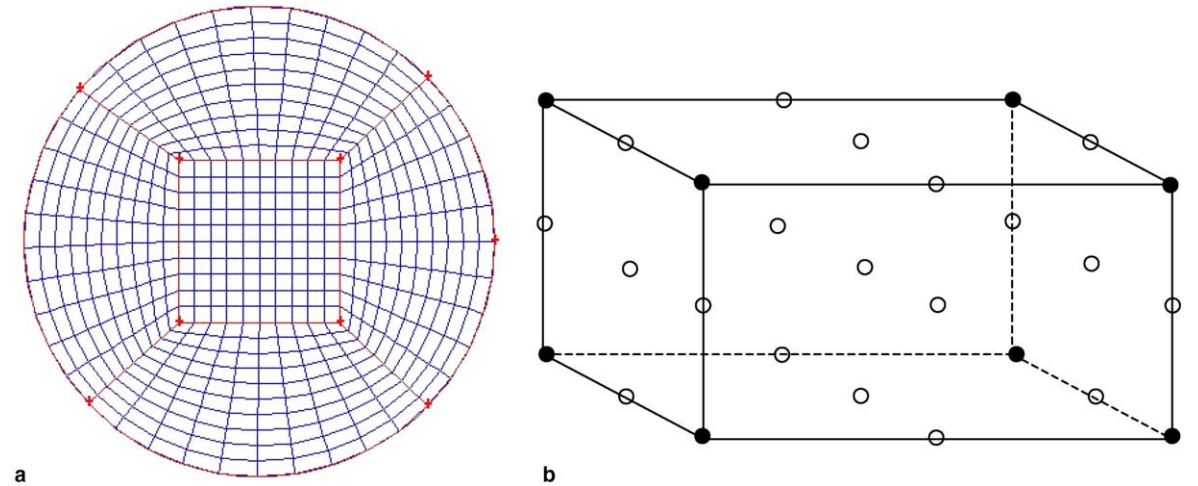

Fig. 3. Grids and nodes: (a) unstructured grid on one cross-section of the helical pipe and (b) nodes used for storage of dependent variables in the three-dimensional element.

of the predicted results at different grid distributions (sectional × axial) for a fully developed laminar fluid flow in coiled tube. The sectional number refers to the total number of elements on one cross-section (φ = constant) of the pipe. Table 1 indicates that the 500×240 grid arrangement ensures a satisfactory solution for heat transfer in helical tubes. With the 500×240 and even finer grids, some computations were also repeated for fluid flow and heat transfer in helical pipes at lower δ, higher Reynolds number. It was observed that there was particularly no difference in the values of Nusselt number and friction factor.

4. Results and discussion

Axial flow developments were obtained at different planes $\phi = 15°$ (inlet), 30°, 60°, 120°, 340° for straight helix and coiled flow inverter. The temperature profiles were also reported at the same planes. The fully developed profiles are introduced at the inlet of the geometry. The Reynolds number is varied from 7 to 400 and the Prandtl number is varied from 0.74 to 150 (curvature ratio, $\delta = 1/10$). The physical properties during the simulation were kept constant.

4.1. Description of velocity fields

Figs. 4–6 represents the development of velocity field at different axial positions in the straight helix and chaotic configuration with one and two bends, respectively. The velocity fields are visualised by isotachs of the axial components. Fig. 4 shows that the velocity fields in the straight helix is almost fully developed at $\varphi = 180°$, since there are only minor changes in velocity fields at $\varphi = 270°$ and $\varphi = 340°$. The velocity field is characterized by two longitudinal Dean-type vortices and the axial velocity contours show the familiar C-shape. It can also be seen from Fig. 4 that the maximum velocity is shifted towards the outer wall of the helical coil. Fig. 5 shows that the velocity fields first break than reassemble into Dean roll-cells and the flow is inverted by 120° first and than reassemble at 90°. Therefore a complete 90° inversion is obtained at $\varphi = 180°$. The numerical results of the present study have shown that velocity fields on any cross-section after fully developed flow in bent coil configuration is almost identical as those of straight helical tube under the present investigated conditions. The above result reveals that the velocity contours, which are having maximum value in straight helix, after inversion will be having minimum value and the velocity vectors, which are having minimum value before bend, are now having maximum value after 90° bend. Therefore the radial mixing between the fluid elements is much higher than that of straight tube and straight helix. The velocity contours are again inverted by 90°, after the second bend as shown in Fig. 6, the same phenomenon was observed as discussed in Fig. 5.

The complete axial velocity profiles for helical pipe and bend configurations at different angular planes are shown in Figs. 7–9. In the helical pipe, when φ is small, the velocity is almost symmetrical to center point on both horizontal and vertical centerlines. With the increase of φ, the axial velocity becomes asymmetrical. In the horizontal centerline, the maximum velocity shifts to the outside of the pipe because of the unbalanced centrifugal force on the main flow. The velocity fields from outlet of the straight helical tube were introduced at the one-bend configuration $\varphi_1 = 0.0$. From Fig. 8 it can be seen that the flow fields get reoriented due to the 90° bend. Same phenomenon is obtained at 2nd bend as shown in Fig. 9.

The present work is in good agreement with the detailed measurements of Le Guer et al. [20], Castelain [9] and Mokrani et al.[10] and numerical predictions of Duchene et al. [2] in a twisted duct flow. Duchene et al. [2] carried out numerical study of velocity profiles in a twisted duct of square cross-section made up of 90° bends. They reported the similar phenomenon of flow inversion at different bend as observed in the present work. Le Guer et al. [20], Castelain [9] and Mokrani et al. [10] experimentally studied the hydrodynamics of the flow in twisted bends. Their experimental results demonstrated that the flow produces very complex stretching and folding patterns in the velocity profiles.

4.2. Description of temperature fields

The heat transfer in bent coil configuration is higher than the helical coils. The thermal development study was carried out under the condition of constant wall temperature for straight helix and bent coil configuration. Fig. 10 shows the variations of computed temperature contours at various cross-sectional planes in coiled tubes. It may be concluded that with the increase of φ, the secondary velocity is enhanced, and the high temperature zones shift to the outer side because of centrifugal force. The pattern of axial temperature development at various axial distances are clearly related to the fluid mechanics of the systems. For a very short distance from the tube inlet the secondary flow effect is negligible so the temperature profiles in the coiled tube is similar to that in straight tube except for the effect of skewed axial velocity profiles which is to set up a circumferential temperature gradient. The secondary velocity increases very rapidly with increasing distance from the tube wall. Therefore, the thermal boundary layer develops with the increase of axial distance. This temporarily arrests the growth of the thermal boundary layer and the secondary convection transfers the most of the heat into the fluid core. Therefore the temperature profiles become kidney

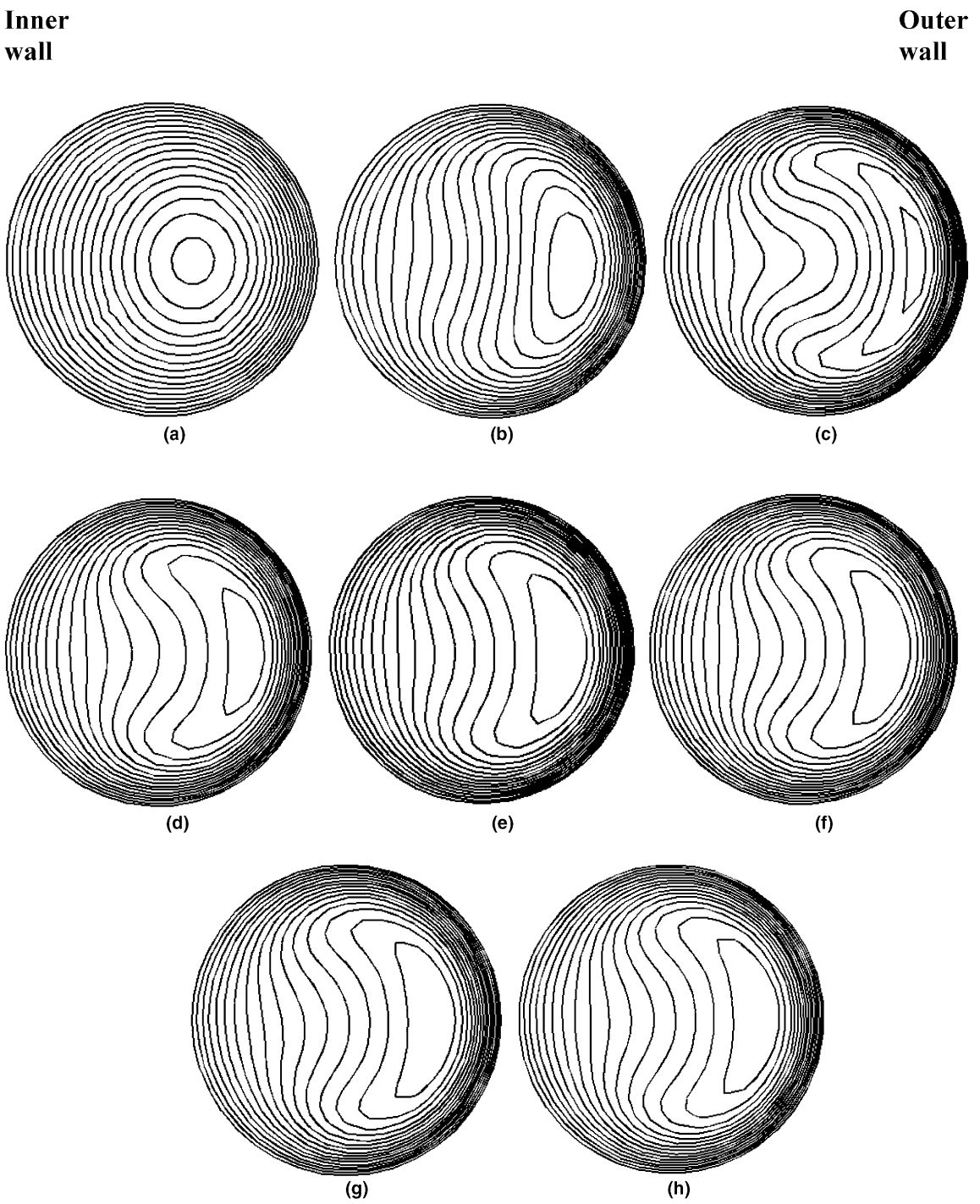

Fig. 4. Computed velocity contours at different cross-sections in coiled tube. (a) $\varphi = 15°$, (b) $\varphi = 30°$, (c) $\varphi = 60°$, (d) $\varphi = 90°$, (e) $\varphi = 120°$, (f) $\varphi = 180°$, (g) $\varphi = 270°$, and (h) $\varphi = 340°$.

shaped and more skewed towards the outer wall of the tube. Therefore according to Raju and Rathna [7] in the helical tube there are cold regions, which can further be modified by using radial mixing in the tube.

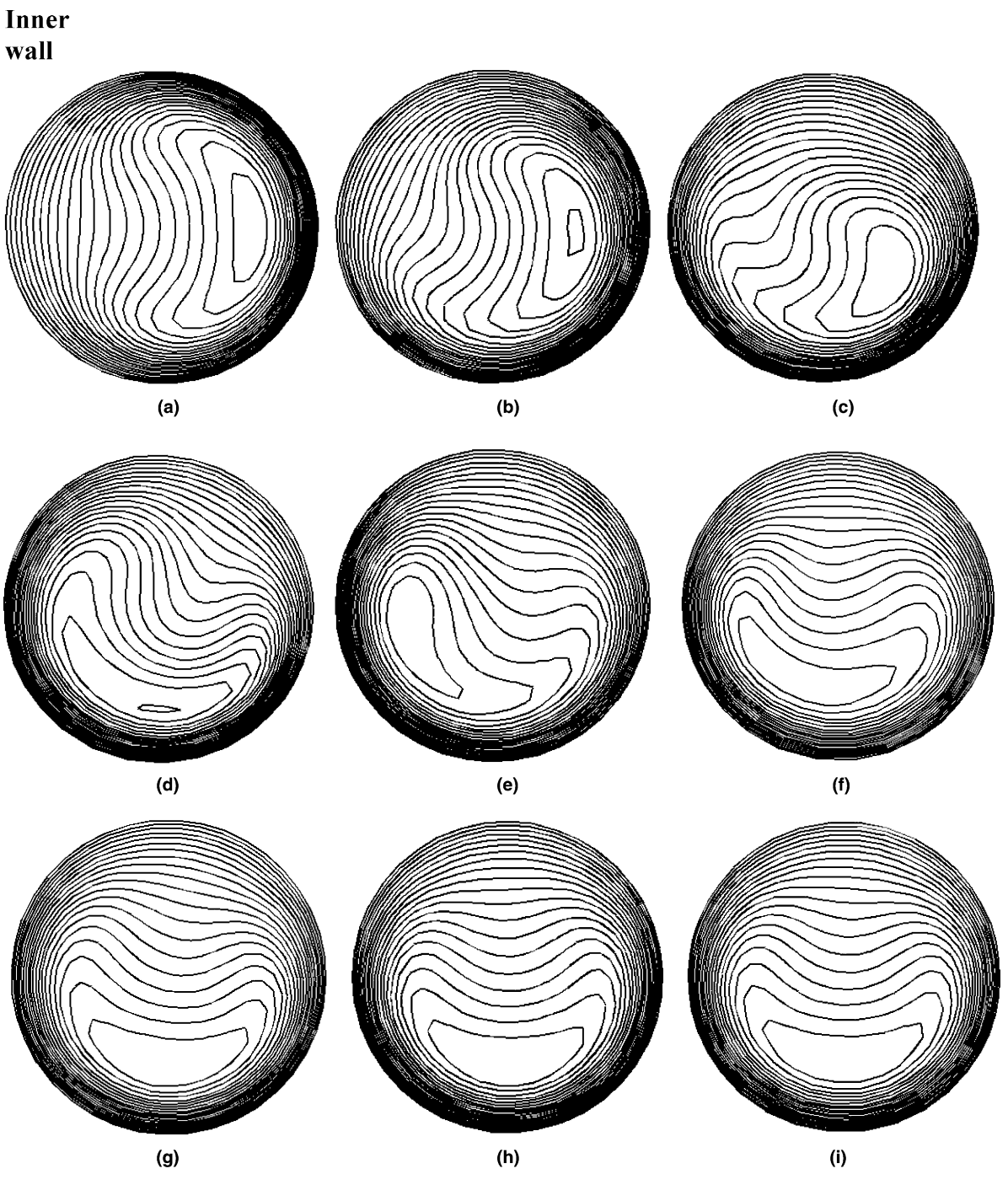

Fig. 5. Computed velocity contours at different cross-sections in bent helix (one-bend). (a) $\varphi = 0°$, (b) $\varphi = 15°$, (c) $\varphi = 30°$, (d) $\varphi = 60°$, (e) $\varphi = 90°$, (f) $\varphi = 120°$, (g) $\varphi = 150°$, (h) $\varphi = 180°$, and (i) $\varphi = 340°$.

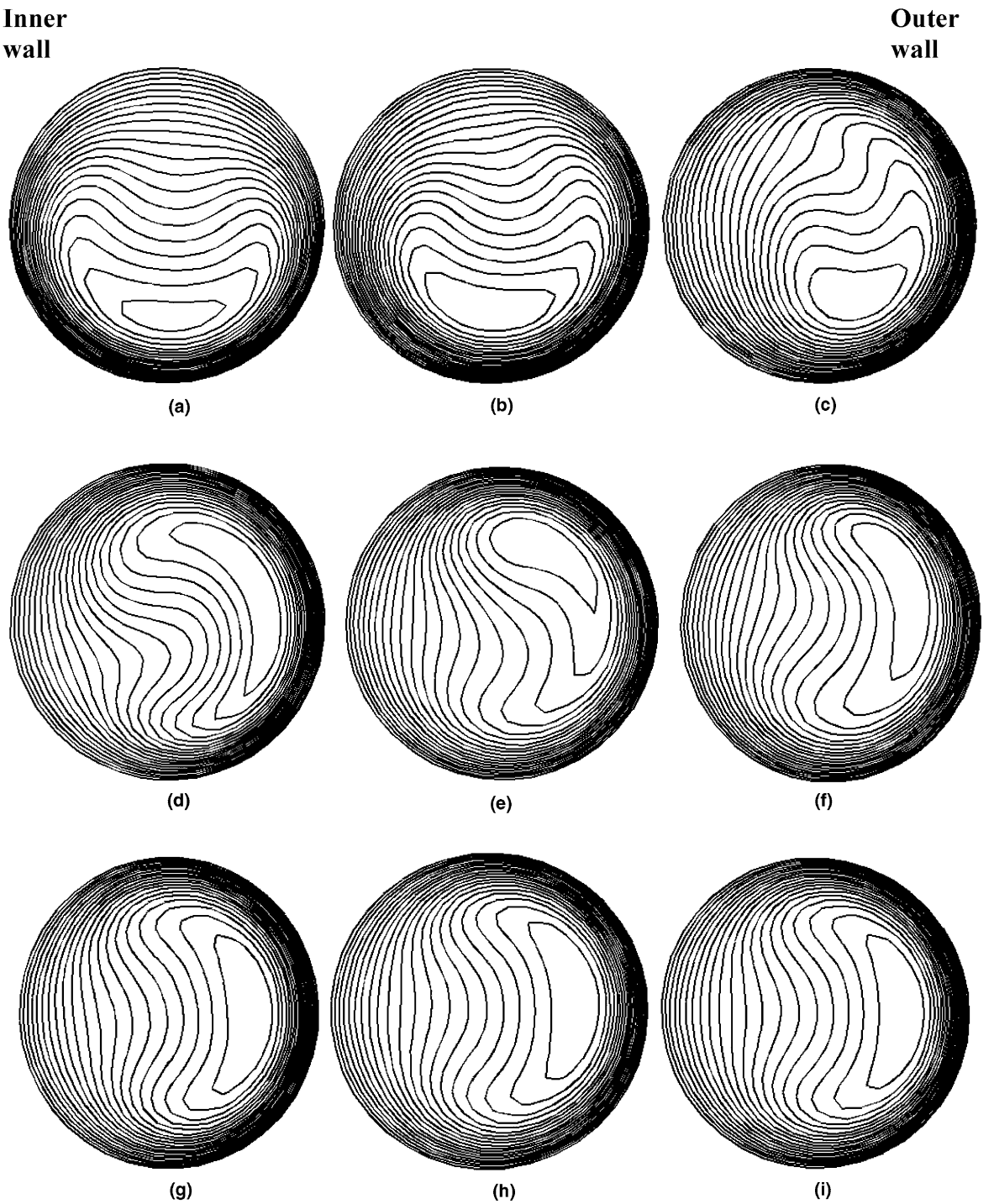

Fig. 6. Computed velocity contours at different cross-sections in bent helix (two-bends). (a) $\varphi = 0°$, (b) $\varphi = 30°$, (c) $\varphi = 60°$, (d) $\varphi = 90°$, (e) $\varphi = 120°$, (f) $\varphi = 150°$, (g) $\varphi = 180°$, and (h) $\varphi = 340°$.

In the present study the thermal profiles were further modified by inserting a 90° bend between the two straight helixes. In Fig. 11 it is shown that, after the introduction of the 90° bend in the helical tube the

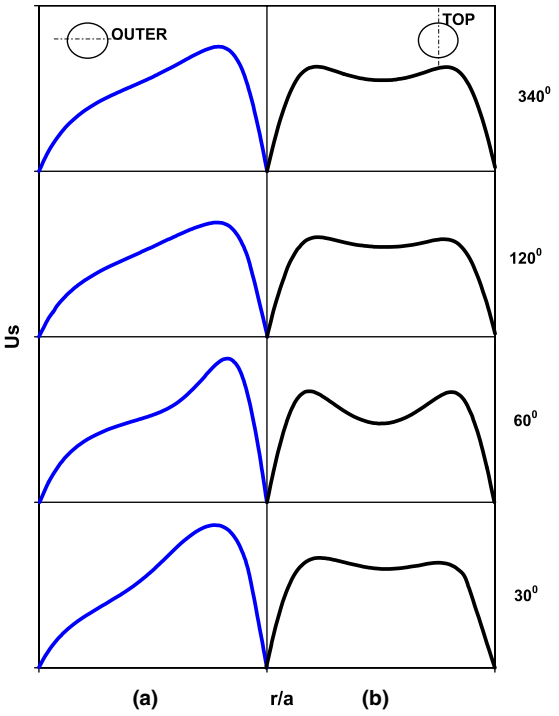

Fig. 7. Developments of axial velocity profile in coiled tube in horizontal centerline (a) and vertical centerline (b), $N_{Re} = 316$, $N_{De} = 100$.

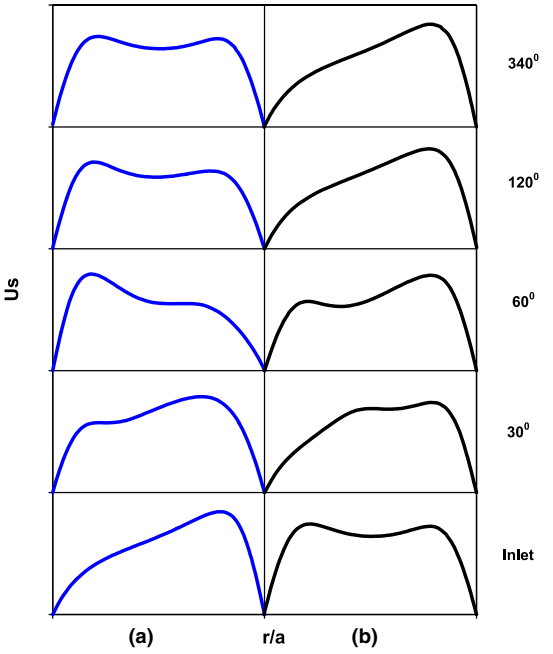

Fig. 8. Developments of velocity profiles at different cross-sections in bent helix (one-bend) in horizontal centerline (a) and vertical centerline (b), $N_{Re} = 316$, $N_{De} = 100$.

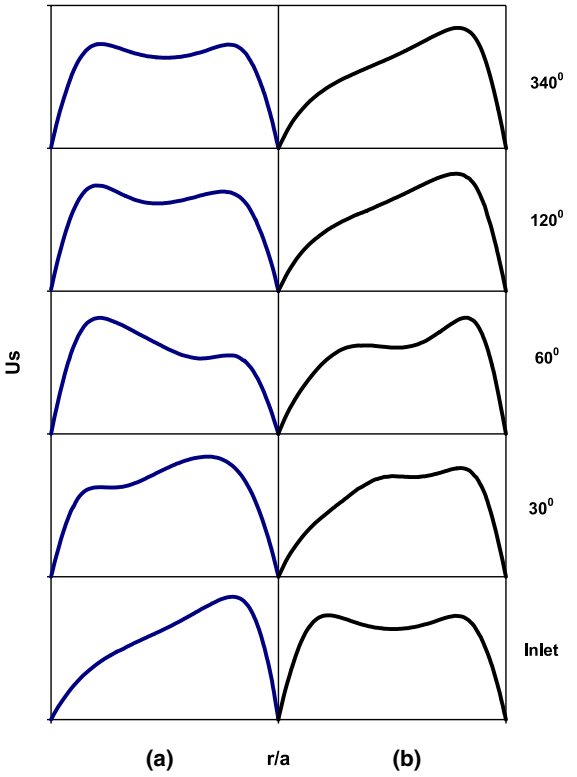

Fig. 9. Developments of velocity profiles at different cross-sections in bent helix (two 90° bend) in horizontal centerline (a) and vertical centerline (b), $N_{Re} = 316$, $N_{De} = 100$.

thermal fields are completely inverted by 90°. The cold regions after the flow inversion got heated and the temperature fields again modified. At the second bend, same phenomena is repeated as obtained at the first bend (Fig. 12). The main difference between the helical and the bent coil configuration can be qualitatively described from their temperature profiles. In the helical coils the Dean roll cells transport hot fluid elements from the neighbourhood of the wall to the center of the tube. However the fluid elements trapped in the center of the Dean roll cells were prevented from approaching the hot wall. Consequently the centerline of the tube was overheated and the center of the Dean roll cells were not heated enough. Therefore the heat transfer phenomenon in the helical coil was not very high. The Dean roll cells were also locally present after the bend, but after each curvature plane the centrifugal force was reoriented, so the Dean roll-cells of the previous arm vanished and reappeared in a plane perpendicular to the previous plane. Fluid elements that were trapped in the Dean roll-cells of the next bend so that more fluid elements can visit hot regions close to the walls. The consequence of this phenomenon is the homogenization of heating in bent coils.

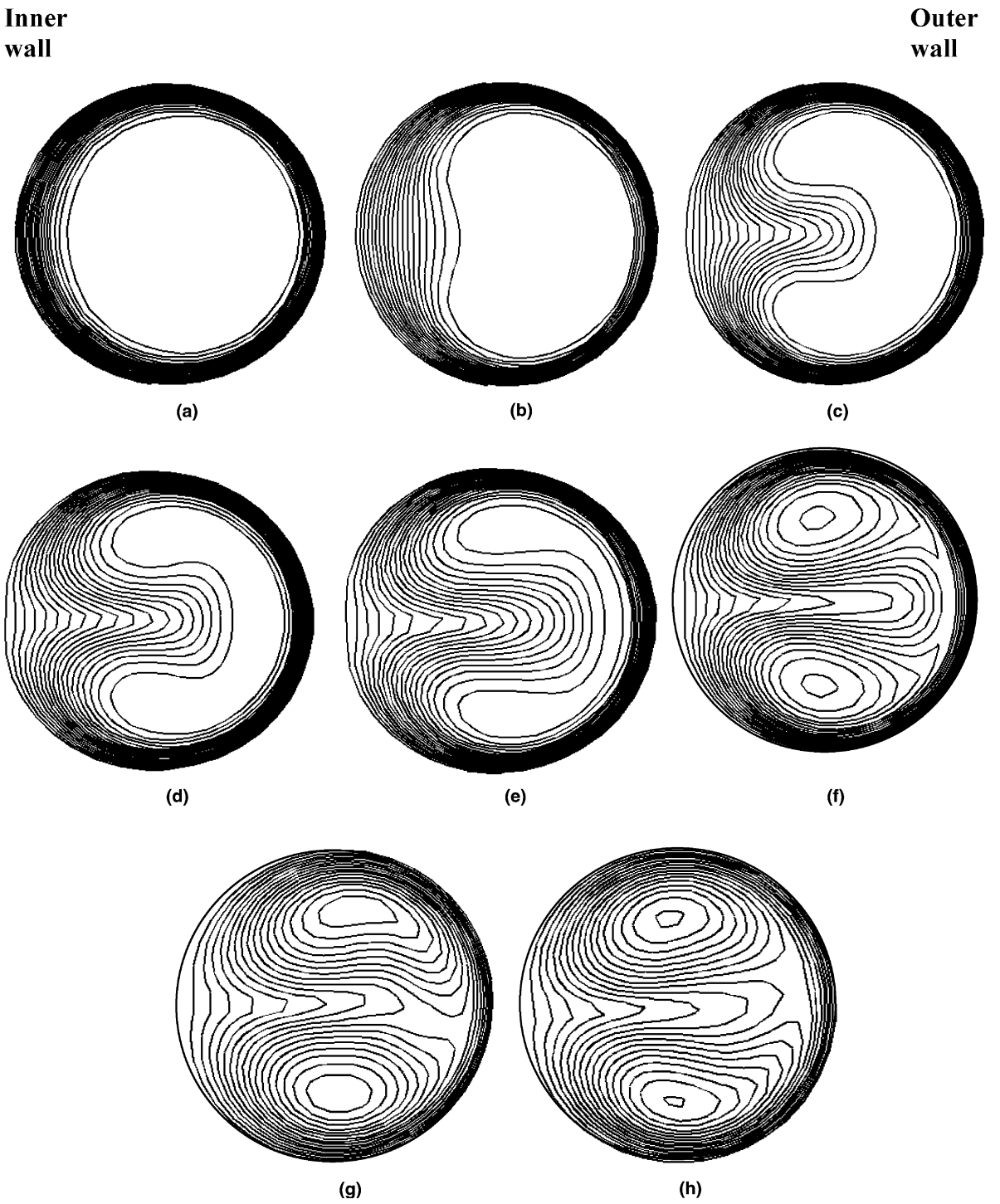

Fig. 10. Computed temperature contours at different cross-sections in coiled tube. (a) $\varphi = 15°$, (b) $\varphi = 30°$, (c) $\varphi = 60°$, (d) $\varphi = 90°$, (e) $\varphi = 120°$, (f) $\varphi = 180°$, (g) $\varphi = 270°$, and (h) $\varphi = 340°$.

Figs. 13 and 14 show the development of non-dimensional temperature (Θ) fields in helical pipes and chaotic configuration at different axial positions. When the axial distance, φ, is small, fluid of uniform temperature

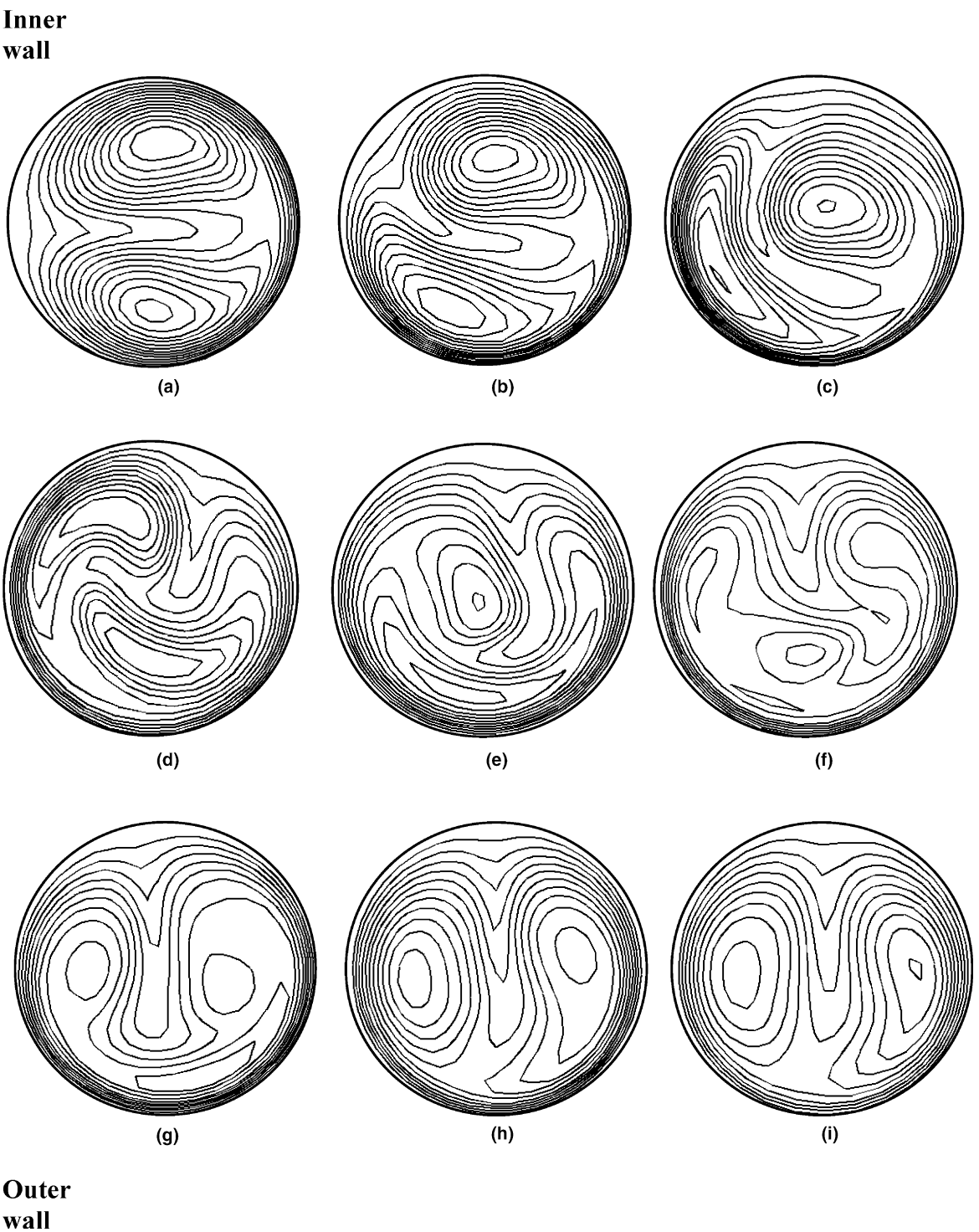

Fig. 11. Computed temperature contours at different cross-sections in bent helix (one bend). (a) $\varphi = 0°$, (b) $\varphi = 15°$, (c) $\varphi = 30°$, (d) $\varphi = 60°$, (e) $\varphi = 90°$, (f) $\varphi = 120°$, (g) $\varphi = 150°$, (h) $\varphi = 180°$, and (i) $\varphi = 340°$.

occupies most of the area of the cross-section. As φ increases, the unbalanced centrifugal force of the main flow results in the shift of point of the maximum Θ to outside of the pipe, forming steeper Θ gradient near

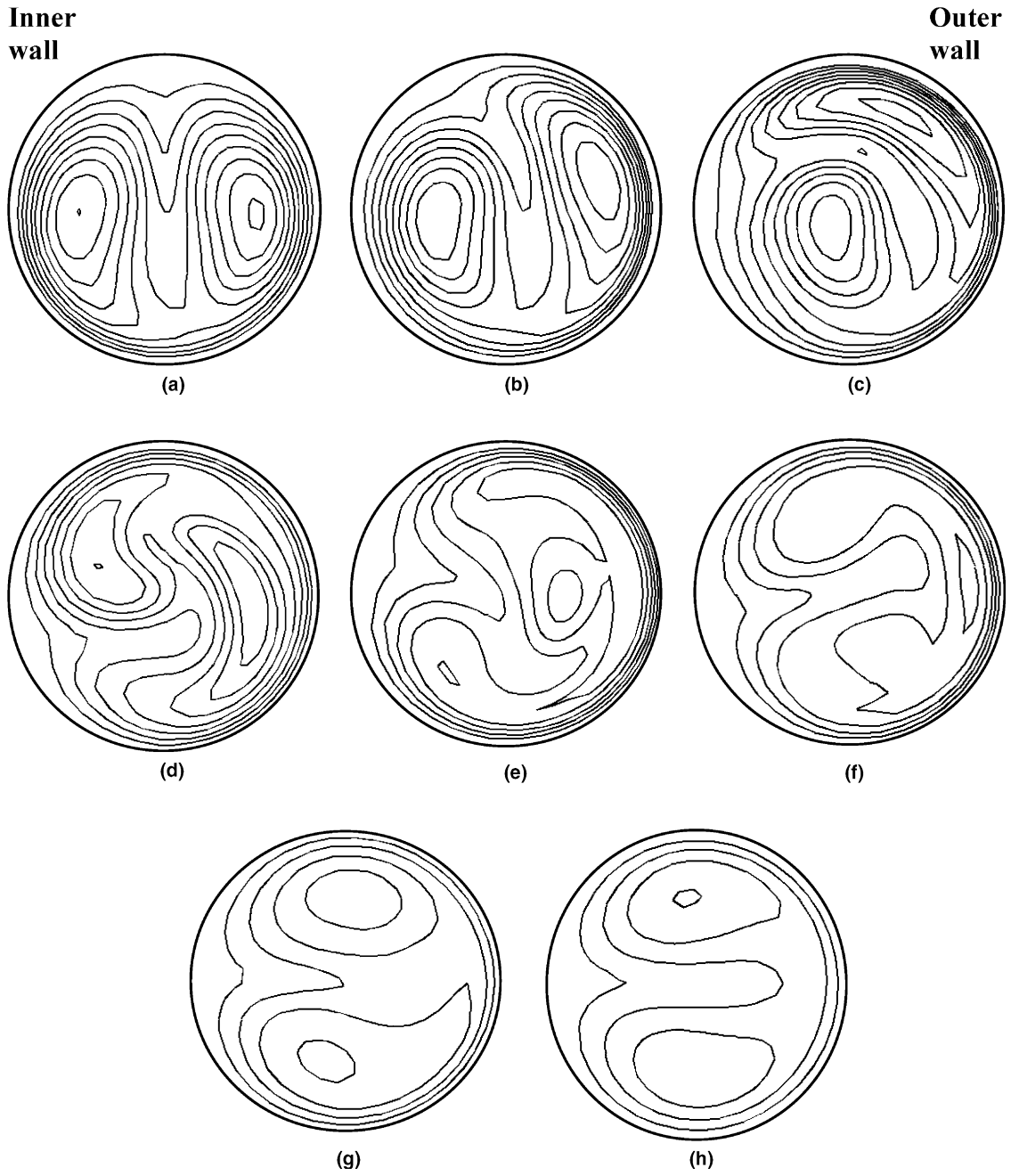

Fig. 12. Computed temperature contours at different cross-sections in bent helix (two-bend). (a) $\varphi = 0°$, (b) $\varphi = 15°$, (c) $\varphi = 30°$, (d) $\varphi = 60°$, (e) $\varphi = 90°$, (f) $\varphi = 120°$, (g) $\varphi = 150°$, (h) $\varphi = 180°$, and (i) $\varphi = 340°$.

the outer wall. When the heat transfer is fully developed, both the position shift and the magnitude of the maximum Θ reach their maximum value. As shown in Fig. 13, the maximum temperature is obtained at the outer wall of the tube and minimum at the inner wall of the tube.

4.3. Effect of number of bends

Figs. 15 and 16 show the velocity fields and temperature fields by varying the number of bends. Fig. 15 shows that, after the fully developed flow there is no difference in the velocity fields in helical tube and different

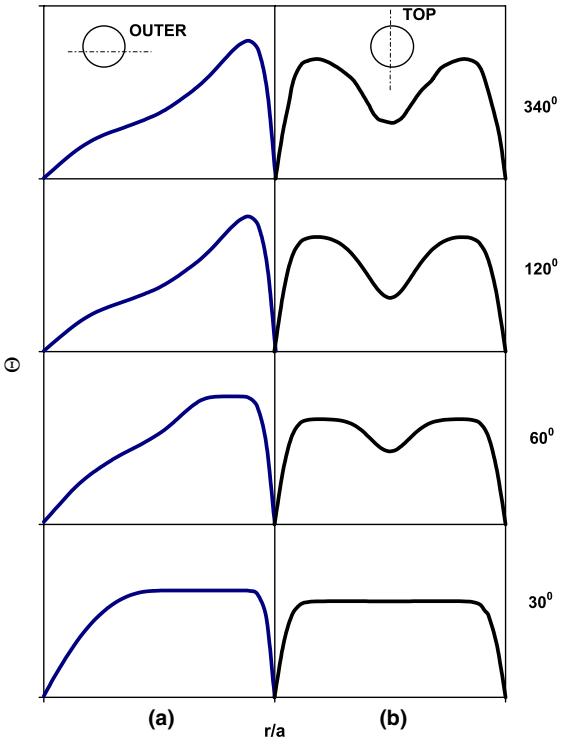

Fig. 13. Development of temperature profile in coiled tube in horizontal centerline (a) and vertical centerline (b), at $N_{Re} = 316$, $N_{De} = 100$.

bent coil configurations in the horizontal as well as vertical centerline. Fig. 16 shows that the maximum Θ gradient value is for different configurations. The temperature fields are modified at every bend and enhance heat transfer in the bent coil configuration. In the vertical centerline there is no change in temperature profiles.

5. Heat transfer enhancement

5.1. Data comparison

In order to predict the enhancement of heat transfer in the proposed innovative bent coil configuration, the present computation technique was checked for its reliability and accuracy by comparing the literature value of fully developed heat transfer coefficient in helical coiled tubes. Fig. 17 illustrates the comparison of present predictions of the fully developed Nusselt number with Manlapaz and Churchill's [27] correlation

$$N_{Nu} = \left[\left(3.657 + \frac{4.343}{\left(1 + \frac{957}{N_{Pr} N_{He}^2}\right)^2} \right)^3 + 1.158 \left(\frac{N_{He}}{1 + \frac{0.477}{N_{Pr}}} \right)^{3/2} \right]^{1/3} \quad (9)$$

It can be observed from Fig. 17 that the present predictions of Nusselt number were in good agreement with the available results. The maximum deviation between the present predictions and the empirical correlation is less than 5% within the examined parameter range.

The results of the numerical computations for enhancement of heat transfer with Dean number (N_{De}) and Prandtl number (N_{Pr}) are shown in Fig. 18(a) and (b), respectively, in a bent coil configuration having seven 90° bends. Fig. 18(a) shows the influence of Dean number on the enhancement of heat transfer in bent coil configuration, as the Dean number increases Nusselt number increases. It can also be observed that there is 20–30% heat transfer enhancement in bent coil configuration in terms of the fully developed Nusselt number (N_{Nu}) as compared to the straight coil.

The Prandtl number is also seen to have an effect similar to the Dean number (Fig. 18(b)). The enhanced mixing occurring in the case of the bent coil configuration is a result of convective motion which is strong compared to thermal diffusion for the fluids with high Prandtl number. For fluids with low Prandtl number, diffusion tends to smear out the temperature profile and reduces the effective contribution of the convective transfer. It can be seen from Fig. 18(b) that at low Prandtl number ($N_{Pr} = 7$), there is 35% enhancement in heat transfer while at higher Prandtl number ($N_{Pr} = 100$) the enhancement is 70% in the bent coil configuration as compared to the straight helix.

Efforts have also been made to predict the variation of friction factor with Dean number and are reported in Fig. 18(c) It can be seen from Fig. 18(c) that at low values of Dean numbers, there is not much difference between the friction factor in coiled tube and bent coil configuration. As the Dean number increases the difference in friction factor between the coiled tube and bent coil configuration increases.

Fig. 19 shows the enhancement in heat transfer and relative increase in the pressure drop. The enhancement in heat transfer was estimated by calculating the ratio of heat transfer in bent coil configuration to the straight helix. Similarly in case of pressure drop, the ratio of pressure drop in the bent coil configuration to the straight helix was reported. It can be observed from Fig. 19 that there is an enhancement of 20–30% in heat transfer and the relative pressure drop is 5–6%.

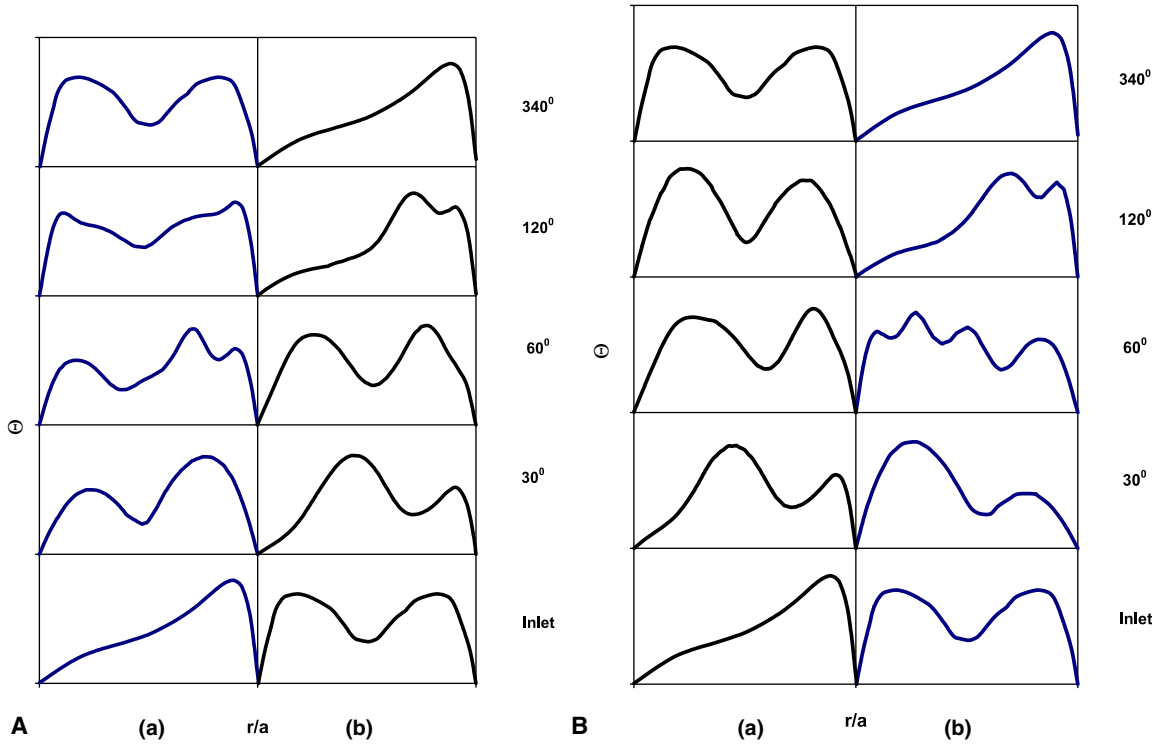

Fig. 14. (A) Developments of temperature profile in bent helix (one 90° bend) in horizontal centerline (a) and vertical centerline (b) $N_{Re} = 316$, $N_{De} = 100$. (B) Developments of temperature profile in bent helix (two 90° bend) in horizontal centerline (a) and vertical centerline (b), $N_{Re} = 316$, $N_{De} = 100$.

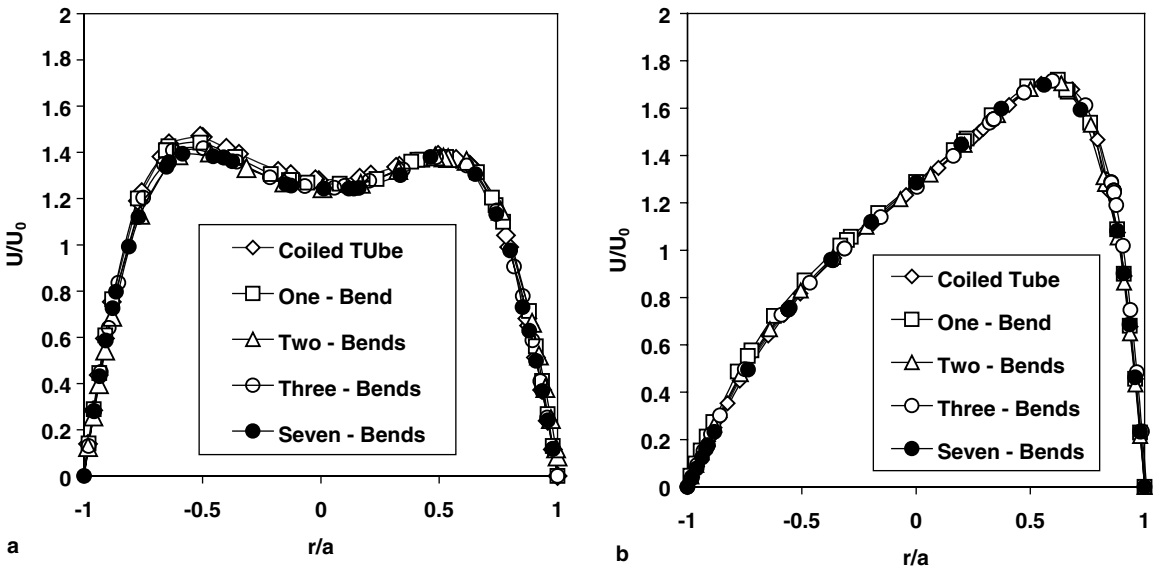

Fig. 15. Developments of axial velocity profile in coiled tube and bend configuration in horizontal centerline (a) and vertical centerline (b), $N_{Re} = 316$, $N_{De} = 100$ at $\phi = 360°$.

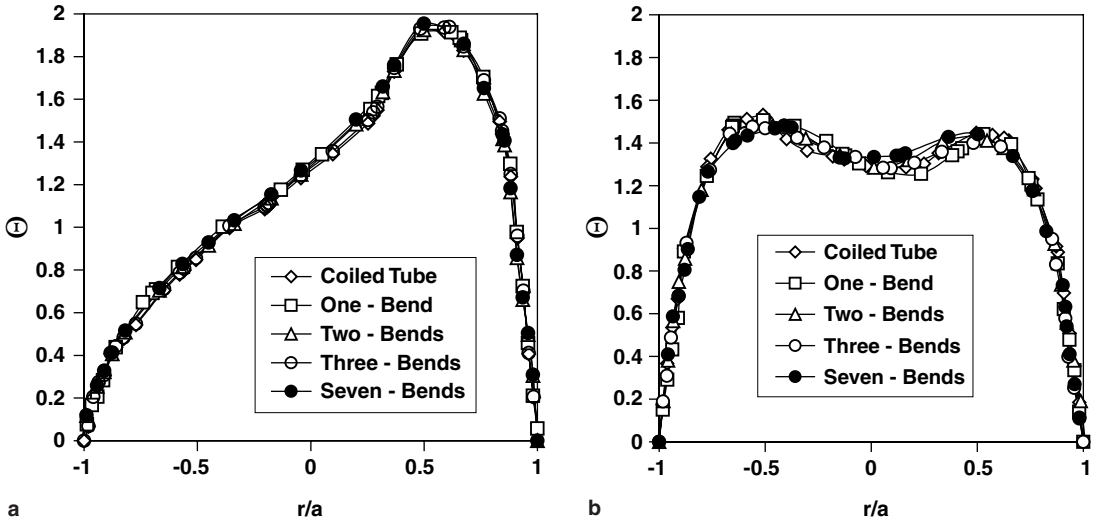

Fig. 16. Developments of temperature profile in coiled tube and bend configuration in horizontal centerline (a) and vertical centerline (b), $N_{Re} = 316$, $N_{De} = 100$ at $\phi = 360°$.

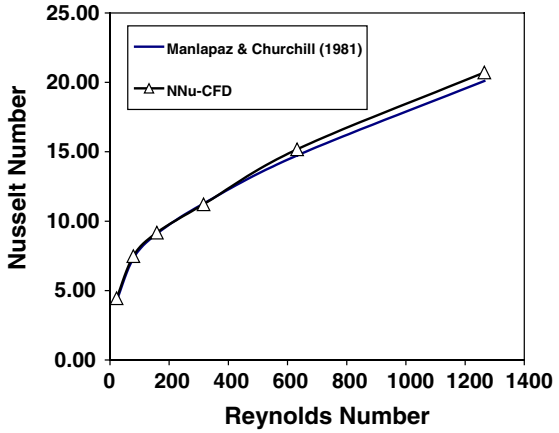

Fig. 17. Comparison of Nusselt number in coiled tubes using computational fluid dynamics and Manlapaz and Churchill's [27] correlation at $N_{Pr} = 7$.

6. Conclusions

Three-dimensional developing flows and heat transfer in helical tubes and bent coil configuration (chaotic configuration) has been numerically simulated with a control-volume finite difference method (CVFDM). In the helical or regular coils, Dean roll cells generate confined regions in the tube cross-section in which fluid elements trapped inside Dean roll-cells stay trapped from the entrance to the exit of the helical coils: they can escape these closed zones only by diffusion. This segregation causes zones of overheating separated by regions of no heating and hence a non-uniform temperature in the tube cross-section.

A new innovative device of the bent coil configuration is presented; inspired by the work of Saxena and Nigam [22,23] by changing the direction of flow in a flow system. The basic geometry of the tube coil is constituted from an ensemble of coils and bends. The curvature plane of each bend makes 90° angle with those of neighboring plane. Dean roll-cells generated in the bend are the building blocks of a stretching and folding process that increases radial mixing in the fluid, thus enhancing heat transfer. From the study it was observed that the Dean roll cells generated in the bent coil configuration are locally similar in helical tube after fully developed flow. However, their effects on convective heat transfer between the tube wall and fluid are quite different. In the coiled flow inverter, the Dean roll-cells smear temperature differences in the tube cross-section and, therefore, render it uniform. The flatter temperature distribution in the bent coil configuration is attributed to the radial mixing of fluid elements due to the flow inversion at the 90° bends, which contributes also to the enhancement of the global efficiency of a bent coil heat exchanger as compared to regular coils. Aside from the high thermal efficiency of bent coil configuration, the low mechanical stresses due to the laminar nature of the flow and uniform temperature distribution could be of significant benefit in process industry. The bent coil configuration also displays a heat transfer enhancement of 20–30% in terms of the fully developed Nusselt numbers compared to the straight coil over a range of $25 \leqslant N_{Re} \leqslant 1200$ with little change in the pressure drop.

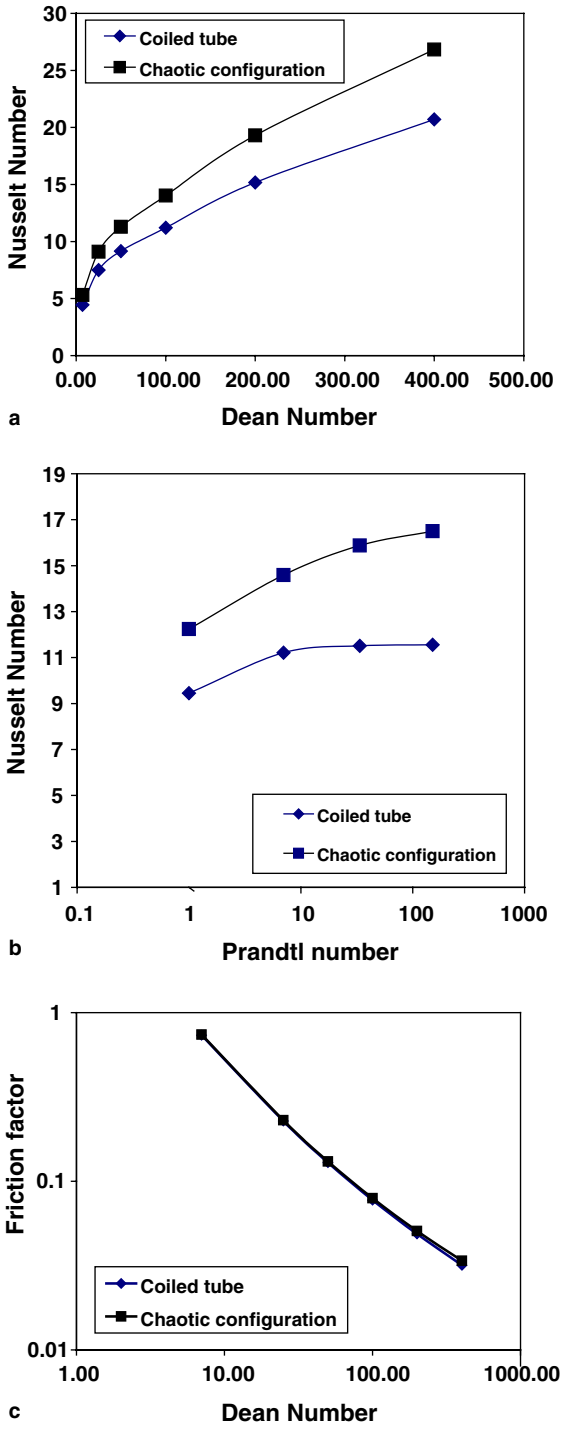

Fig. 18. (a) Nusselt number variation with Reynolds number at $N_{Pr} = 7.0$ and $\delta = 0.1$; (b) Nusselt number variation with Prandtl number at $N_{Re} = 316$ and $\delta = 0.1$; and (c) friction factor variation with Reynolds number at $N_{Pr} = 7.0$ and $\delta = 0.1$ in bent coil configuration, coiled tube and straight tube.

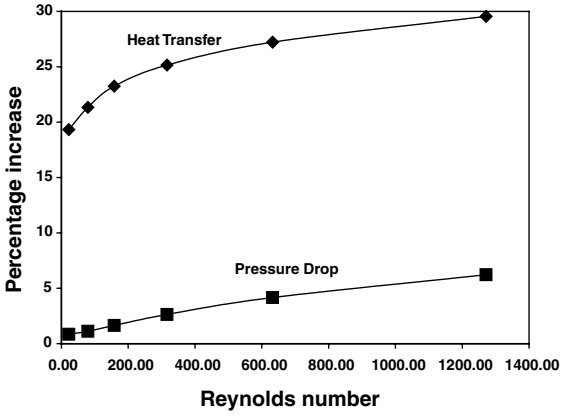

Fig. 19. Relative increase in heat transfer and relative pressure drop in bent coil configuration.

Acknowledgement

The authors gratefully acknowledge the Ministry of Chemical and Fertilizers, GOI, India for funding the project.

References

[1] S.W. Jones, O.M. Thomas, H. Aref, Chaotic advection by laminar flow in twisted pipe, J. Fluid Mech. 209 (1989) 335–357.
[2] Ch. Duchene, H. Peerhossaini, P.J. Michard, On the velocity field and tracer patterns in a twisted duct flow, Phys. Fluids 7 (1995) 1307–1317.
[3] S.A. Berger, L. Talbot, L.S. Yao, Flow in curved pipes, Ann. Rev. Fluid Mech. 15 (1983) 461–512.
[4] R.K. Shah, S.D. Joshi, Convective heat transfer in curved ducts, in: S. Kakac, R.K. Shah, W. Aung (Eds.), Handbook of Single-Phase Convective Heat Transfer, Wiley, New York, 1987 (Chapter 5).
[5] W.R. Dean, Note on the motion of fluid in a curved pipe, Philos. Mag. 4 (1927) 208–223.
[6] W.R. Dean, The streamline motion of fluid in a curved pipe (second paper), Philos. Mag. 7 (5) (1928) 673–695.
[7] K.K. Raju, S.L. Rathna, Heat transfer for flow of a power law fluid in a curved pipe, J. Indian Inst. Sci. 52 (1970) 34–37.
[8] H. Peerhossaini, C. Castelain, Y. Le Guer, Heat exchanger design based on chaotic advection, Exp. Therm. Fluid Sci. 7 (1993) 333–344.
[9] A. Mokrani, C. Castelain, Y. Le Guer, H. Peerhossaini, Mesure du compartment chaotique des trajectories produites dans un ecoulementde Dean alterneen regimelaminaire, Rev. Gen. Therm. 37 (1998) 459–474.
[10] A. Mokrani, C. Castelain, H. Peerhossaini, The effects of chaotic advection on heat transfer, Int. J. Heat Mass Transfer 40 (13) (1997) 3089–3104.

[11] Chagny, C. Castelain, H. Peerhossaini, Chaotic heat transfer for heat exchanger design and comparison with a regular regime for a large range of Reynolds numbers, Appl. Therm. Eng. 20 (2000) 1615–1648.
[12] N. Acharya, M. Sen, H.C. Cheng, Heat transfer enhancement in coiled tubes by chaotic mixing, Int. J. Heat Mass Transfer 35 (10) (1992) 2475–2489.
[13] N. Acharya, M. Sen, H.C. Chang, Applications of chaotic heat and mass transfer enhancement, AIChE Symp. Ser. 286 (88) (1992) 44–49.
[14] Y. Le Guer, H. Peerhossaini, Order breaking in Dean flow, Phys. Fluids A 3 (5) (1991) 1029–1032.
[15] H. Aref, Stirring by chaotic advection, J. Fluid Mech. 143 (1984) 1–21.
[16] C. Castelain, A. Mokrani, P. Legentilhomme, H. Peerhossaini, Residence time distribution in twisted pipe flow: helically coiled system and chaotic, Exp. Fluids 22 (1997) 359–368.
[17] H. Peerhossaini, Y. Le Guer, Effect of curvature plane orientation on vortex distortion in curved channel flow, in: C.D. Andereck, F. Hayot (Eds.), Ordered and Turbulent Patterns in Taylor–Couette Flow, Plenum Press, New York, 1992, pp. 263–272.
[18] H. Peerhossaini, Y. Le Guer, Chaotic motion in the Dean instability flow—a heat exchanger design, Bull. Am. Phys. Soc. 35 (1991) 2229.
[19] C. Castelain, D. Berger, P. Legentilhomme, A. Mokrani, H. Peerhossaini, Experimental and numerical characterization of mixing in a steady spatially chaotic flow by means of residence time distribution measurements, Int. J. Heat Mass Transfer 43 (2000) 3687–3700.
[20] C. Castelain, A. Mokrani, Y. Le Guer, H. Peerhossaini, Experimental study of chaotic advection regime in a twisted duct flow, Eur. J. Mech. B—Fluids 20 (2001) 205–232.
[21] T. Lemenand, H. Peerhossaini, A thermal model for prediction of the Nusselt number in a pipe with chaotic flow, Appl. Therm. Eng. 22 (2002) 1717–1730.
[22] A.K. Saxena, K.D.P. Nigam, Coiled configuration for flow inversion and its effect on residence time distribution, AIChE J. 30 (1984) 363–368.
[23] K.D.P. Nigam, A.K. Saxena, Residence time distribution in straight and cured tubes, in: N.P. Cheremishinoff (Ed.), Ency. Fluid Mech., 1, Gulf Publishing, USA, 1986, pp. 675–762.
[25] S.V. Patankar, Numerical Heat Transfer and Fluid Flow, Hemisphere, Washington, DC, 1980.
[26] Fluent Users Guide, version 4.4, Fluent Inc., Lebanon, NH, 1996.
[27] R.L. Manlapaz, S.W. Churchill, Fully developed laminar flow in helically coiled of finite pitch, Chem. Eng. Commun. 7 (1980) 57–78.